

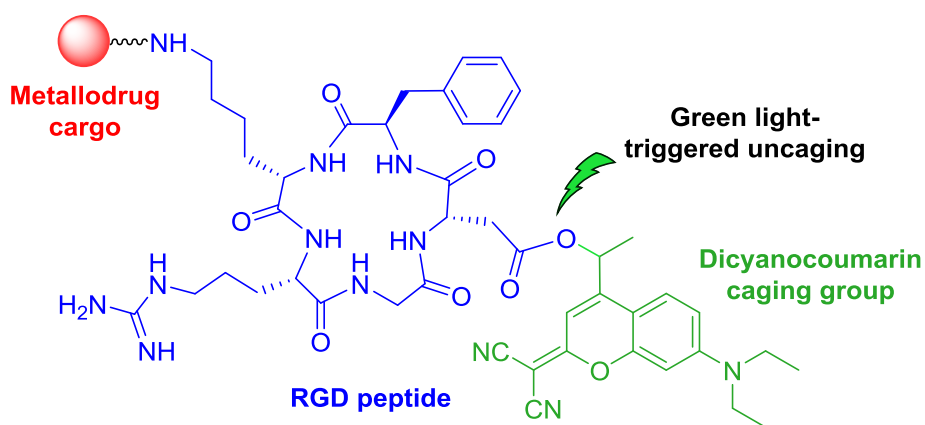
A green light-triggerable RGD peptide for photocontrolled targeted drug delivery: synthesis and photolysis studies

Albert Gandioso,[†] Marc Cano,[†] Anna Massaguer[‡] and Vicente Marchán^{*,†}

[†]Departament de Química Inorgànica i Orgànica, Secció de Química Orgànica, IBUB,
Universitat de Barcelona, E-08028 Barcelona (Spain)

[‡]Departament de Biologia, Universitat de Girona, E-17071 Girona (Spain)

TOC ABSTRACT GRAPHIC



ABSTRACT

We describe for the first time the synthesis and photochemical properties of a coumarin-caged cyclic RGD peptide, and demonstrate that uncaging can be efficiently performed with biologically-compatible green light. This was accomplished by using a new dicyanocoumarin derivative (DEAdcCE) for the protection of the carboxyl function at the side chain of the aspartic acid residue, which was selected on the basis of Fmoc-tBu SPPS compatibility and photolysis efficiency. The shielding effect of a methyl group incorporated in the coumarin derivative near the ester bond linking both moieties in combination with the use of acidic additives such as HOBt or Oxyma during the basic Fmoc-removal treatment was found to be very effective for minimizing aspartimide-related side-reactions. In addition, a conjugate between the dicyanocoumarin-caged cyclic RGD peptide and ruthenocene, which was selected as a metallodrug model cargo, has been synthesized and characterized. The fact that green-light triggered photoactivation can be efficiently performed both with the caged peptide and with its ruthenocenoil bioconjugate reveals a great potential for DEAdcCE-caged peptide sequences as selective drug carriers in the context of photocontrolled targeted anticancer strategies.

INTRODUCTION

Light can be used to control where, when and to what extent active species are released from stable, non-biologically active parent molecules.¹ Besides offering a high level of spatiotemporal control, light does not contaminate the living system and its wavelength and intensity can be precisely regulated.² A promising approach consists of introducing photocleavable protecting groups (PPGs or caging groups)^{1b,3} in key positions of the molecule whose biological activity has to be suppressed temporarily. As a result, the active species from the resulting caged compound will be released only upon light irradiation, leading to the expected biological effect at the desired target site. The approach of using caging groups to regulate the activity of molecules with light has found a widespread application¹⁻³ both to cage small compounds⁴ and larger biomolecules such as peptides and proteins⁵ and oligonucleotides.⁶ Caged peptides can be prepared by introduction of PPGs at the side chain of trifunctional amino acids by taking advantage of the amino (Lys), carboxylate (Asp and Glu), thiol (Cys) and hydroxyl (Ser, Thr and Tyr, and their phosphorylated derivatives) functions.⁷ In addition, caging groups have been introduced at the peptide backbone⁸ and, very recently, a bisbipyridyl ruthenium(II) complex has been used to cage histidine residues.⁹ However, most reported peptide caging groups based on organic chromophores (e.g. *o*-nitrobenzyl derivatives or the first-generation of coumarins) require irradiation with shorter wavelengths (UV or blue light) for uncaging, which compromise *in vivo* applications due to their poor capacity of penetration into tissues¹⁰ and known photocytotoxicity.¹¹

Among receptors overexpressed on tumour cells, integrins are particularly attractive targets since they have been linked to tumour angiogenesis, which is an essential process for tumour growth and metastasis.¹² Moreover, integrins are frequently overexpressed in tumour endothelial cells as well as on various tumour cells. Owing to the ability of some integrin subtypes (especially $\alpha_v\beta_3$) to selectively recognize the tripeptide motif -Arg-Gly-Asp-, RGD-containing peptides, particularly the conjugable version of Cilengitide, c(RGDfK), have been used for tumour imaging and for targeted drug delivery of cytotoxic compounds,¹³ including metal-based anticancer agents.¹⁴ In recent years, only few examples of caged versions of RGD peptides have

been described by modifying the Asp residue^{7ce} with a photolabile protecting group or by incorporating an *o*-nitrobenzyl group within the backbone skeleton.^{8a} The fact that such caging groups prevent integrin recognition has been exploited to control integrin-mediated cell adhesion to surfaces by using UV light.

Taking into account the potential of caged peptides in photocontrolled targeted drug delivery therapies and as tools to study of and interfere with complex biological processes,² triggering the uncaging process with wavelengths of light compatible with biological entities is highly appealing. Here we report for the first time the solid-phase synthesis of a cyclic RGD-containing peptide that has been caged at the side chain of the Asp residue with a dicyanocoumarin derivative, which allows photoactivation to be efficiently performed with green light (Figure 1). By synthesizing its ruthenocenoyl conjugate, we have also demonstrated that the uncaging process can be triggered in the presence of a metallodrug model cargo, which opens the door to the use of this caged RGD peptide or other dicyanocoumarin-caged peptide sequences in photocontrolled targeted anticancer therapies.

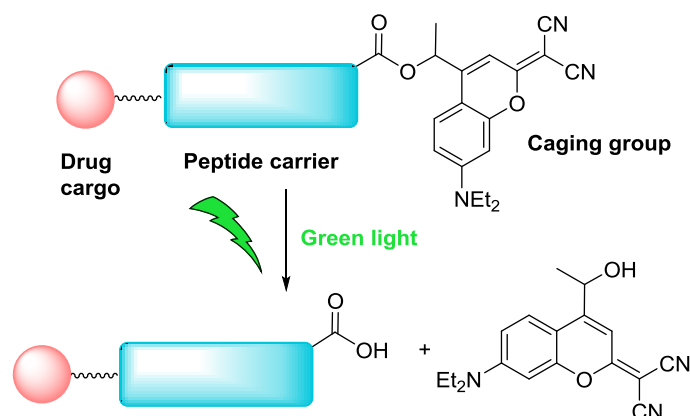


Figure 1. Schematic representation of the uncaging process of a dicyanocoumarin-caged peptide when attached to a drug cargo.

RESULTS AND DISCUSSION

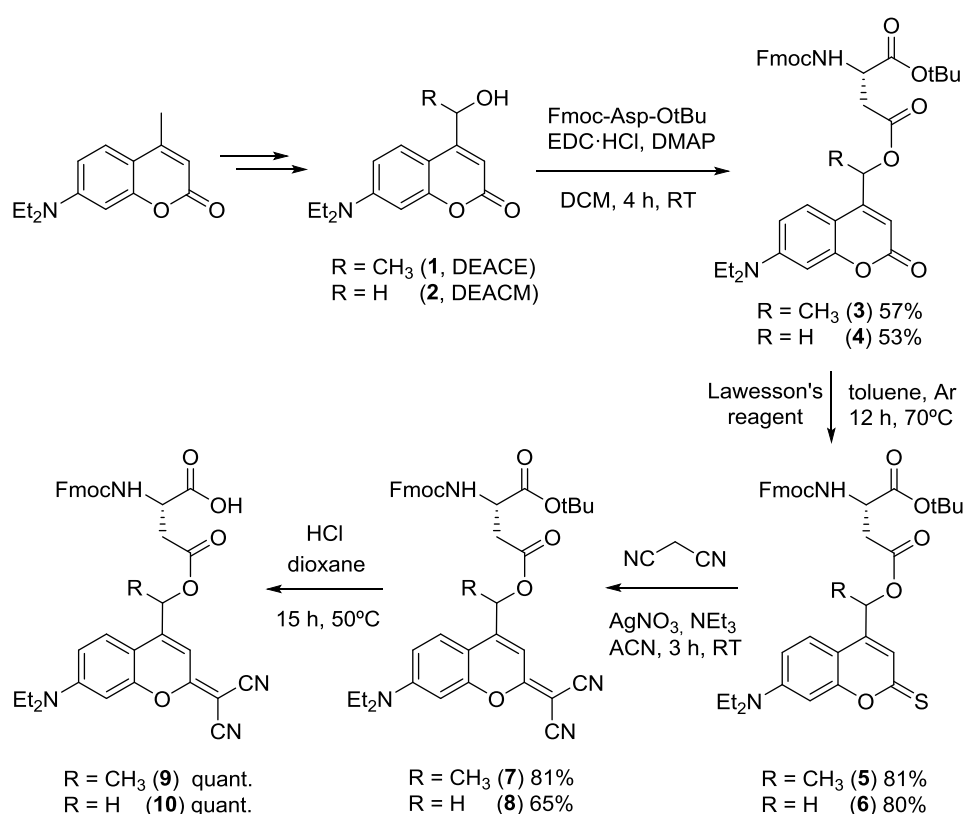
Synthesis and photochemical properties of coumarin-caged Asp derivatives

Coumarinylmethyl derivatives have been used to cage carboxylic acid functions through esterification, being particularly interesting the high red-shifted absorption of the 7-(*N,N*-diethylamino) series.¹⁵ Upon irradiation, a solvent-assisted photolysis produces the free carboxylate from the caged carboxylic acid and a solvent-trapped coumarin as a photoproduct.¹⁶ Recently, del Campo and collaborators^{7e} have found that protection of the side chain of Asp during solid-phase peptide synthesis (SPPS) is more convenient with DEACE coumarin (**1**) than with the classical DEACM (**2**) (Scheme 1).^{7e} The reason relies on the steric hindrance provided by the methyl group incorporated in the coumarin moiety that led to an increase of the stability of the ester bond during the Fmoc-removal basic treatment as compared with the parent DEACM. Based on these precedents, we first focused on modifying the lactone function of the *N*-(9-fluorenylmethoxycarbonyl) (Fmoc)-protected Asp derivatives **3** and **4**^{7e} (Scheme 1) with the aim of studying: 1) if uncaging could be triggered by green light (> 500 nm), and 2) their compatibility with Fmoc-tBu solid-phase peptide synthesis (SPPS) procedures for synthesizing a caged cyclic RGD peptide. As shown in Scheme 1, four new caged Asp derivatives have been synthesized by replacing the carbonyl group of the coumarinyl moiety by thiocarbonyl (**5** and **6**) or by dicyanomethylene (**7** and **8**), since both approaches are known to cause a significant red-shift absorption of the coumarin chromophore^{15b,17} which has been exploited to uncage model carboxylic acids and amines with blue light.

The synthesis of the new Asp monomers (**5-8**) was planned from **3** and **4**, which were prepared from DEACM and DEACE coumarins following previously reported procedures with minor modifications. The synthesis of the thionated derivatives was carried out by reaction with Lawesson's reagent in toluene at 70°C for 12 h. Compounds **5** and **6** were isolated by silica gel column chromatography in good yields (81 and 80%, respectively) and fully characterized by UV-vis, HR-ESI MS and NMR. According to the higher reactivity of the Lawesson's reagent for lactones than for esters,¹⁸ thionation occurred exclusively at the coumarin protecting group (DEACM or DEACE) rather than in the ester or carbamate functions of the amino acid moiety.

Indeed, the chemical shift of the carbonyl group of the lactone in the ^{13}C NMR spectra of **4** (δ : 161.7 ppm) was shifted by *ca* 36 ppm in **6** (δ : 197.0 ppm) due to thionation, and the adjacent proton in ^1H NMR was shifted from 6.1 ppm (**4**) to 7.0 ppm (**6**). Similar effects were observed with compound **5**. The dicyanomethylenecoumarinyl-Fmoc-protected Asp derivatives were obtained by condensation of the respective thionated precursors with malononitrile in the presence of triethylamine and silver nitrate (Scheme 1) in 81% (**7**) and 65% (**8**) yield after silica gel column chromatography and fully characterized by UV-vis, HR ESI MS and NMR. The purity of the amino acid derivatives was also assessed by reversed-phase HPLC (Figure S1 in the Supporting Information). It is worth noting that amino acid derivatives **5** and **7** were isolated as a mixture of two diastereomers due to the additional stereogenic center created by the incorporation of the methyl group at the coumarin skeleton.

Scheme 1. Synthesis of the coumarin-caged Fmoc-protected Asp derivatives (**5-10**).



As a next step the compatibility of the four Asp monomers with Fmoc-tBu SPPS was studied (Figures S2-S5 in the Supporting Information). Unfortunately, thionated monomers were not

completely stable to the TFA cleavage and deprotection conditions, since a considerable amount of desulfurization occurred (about 30% for **5** and 20% for **6**). Both amino acids were also unstable to the typical Fmoc-removing conditions. Reaction of piperidine with the thiolactone was the major side product. By contrast, dicyanomethylenecoumarin-caged Asp monomers (DEAdcCE **7** and DEAdcCM **8**) were found stable to the acid and basic treatments typically used in Fmoc-tBu SPPS (Figures S4-S5), as well as in cell culture medium (DMEM supplemented with 25% fetal bovine serum) after incubation for 1 h at 37°C (Figure S6). The latter is a prerequisite for exploring the biological applications of coumarin-caged peptides. On the basis of the stability studies, we selected dicyanomethylenecoumarin (DEAdcCE and DEAdcCM) as a caging group of Asp and focused on studying the photophysical and photochemical properties of **7** and **8** (see Table 1 and Figures 2 and S7-S10). The UV-vis absorption spectra of both compounds are very similar with an absorbance maximum around 500 nm belonging to π - π^* transitions of the coumarin chromophore. As shown in Table 1, λ_{max} values were slightly red-shifted with respect the corresponding free dicyanocoumarin alcohols (**11** and **14**; the structures are shown in Scheme 2), which correlates with the tendency previously found in other compounds.^{15b} Similarly, the fluorescence emission maxima upon excitation at λ_{max} was also shifted to longer wavelengths in the caged amino acids.

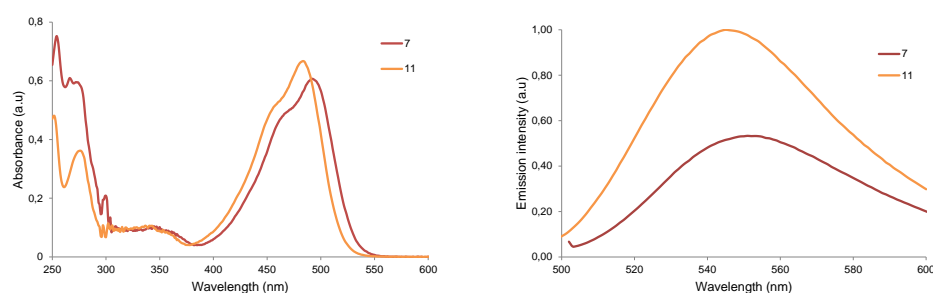


Figure 2. Comparison of the UV-vis spectra (left, 20 μM) and fluorescence emission spectra (right, 50 nM) of DEAdcCE coumarin alcohol (**11**) and of Fmoc-Asp(DEAdcCE)-OtBu (**7**) in Tris buffer pH 7.5/ACN 1:1.

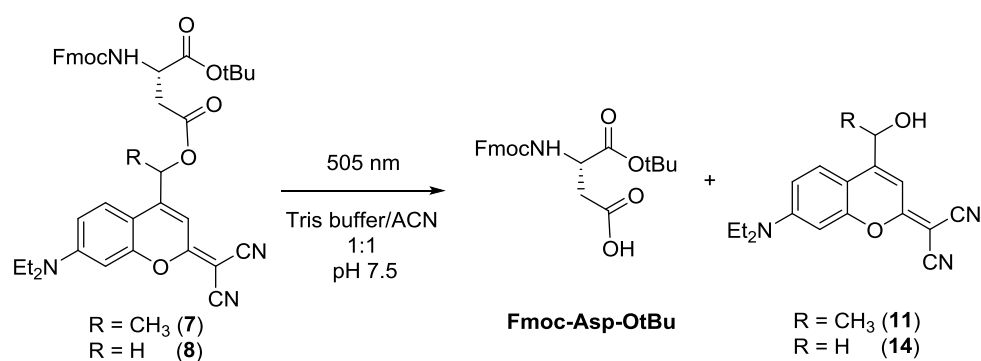
Table 1. Photophysical and photochemical properties of the compounds.

	Absorption		Emission		Uncaging		
	λ_{\max}^a	$\epsilon(\lambda_{\max})^b$	λ_{em}^c	$\Delta\nu^d$	$10^2\phi^e$	$\epsilon(505)^b$	$\epsilon x \phi^f$
7	492	30.3	551	59	0.24	24.5	58
8	489	27.5	555	66	0.10	22.5	22
11	483	33.5	545	62	-	-	-
14	479	28.6	549	70	-	-	-

^aAbsorption maximum (nm); ^bExtinction coefficient at λ_{\max} or at 505 nm ($\text{mM}^{-1} \text{cm}^{-1}$); ^cFluorescence emission maximum upon excitation at λ_{\max} (nm); ^dStokes's shift (nm); ^eQuantum yield for the uncaging process at 505 nm; ^fEfficiency of the uncaging process ($\text{M}^{-1} \text{cm}^{-1}$) (see the Supporting Information).

On the basis of the shape of the absorption curve and of the molar extinction coefficients of both DEAdcCM- and DEAdcCE-caged Asp derivatives at their λ_{\max} and at 505 nm (Table 1), we decided to evaluate if green light could be used to deprotect them efficiently, because it is less harmful to cells and penetrates deeper in tissues than UV or blue light.^{10,11} Photolysis studies were carried out by using a LED as a light source and the course of the uncaging process was monitored by reversed-phase HPLC-ESI MS. As shown in Scheme 2 and in Figures S11-S12, irradiation at 505 nm induced conversion to the uncaged Fmoc-Asp-OtBu and the corresponding coumarin alcohol derivatives in both cases as the main photolytic by-products (**11** from **7** and **14** from **8**). The fact that uncaging of **7** was slightly faster compared with that of **8** (2 min vs 5 min, for a complete deprotection) can be attributed to the higher stability of the secondary carbocation intermediate generated during photoheterolysis¹⁶ of the ester bond of **7**. In good agreement with such photolysis studies, the uncaging quantum yield (ϕ) for **7** was higher than for **8** (Table 1), resulting in a high product ($\epsilon x \phi$), thereby indicating a higher efficiency for the uncaging process.^{1b}

Scheme 2. Photoactivation of dicyanocoumarin-caged Asp monomers.

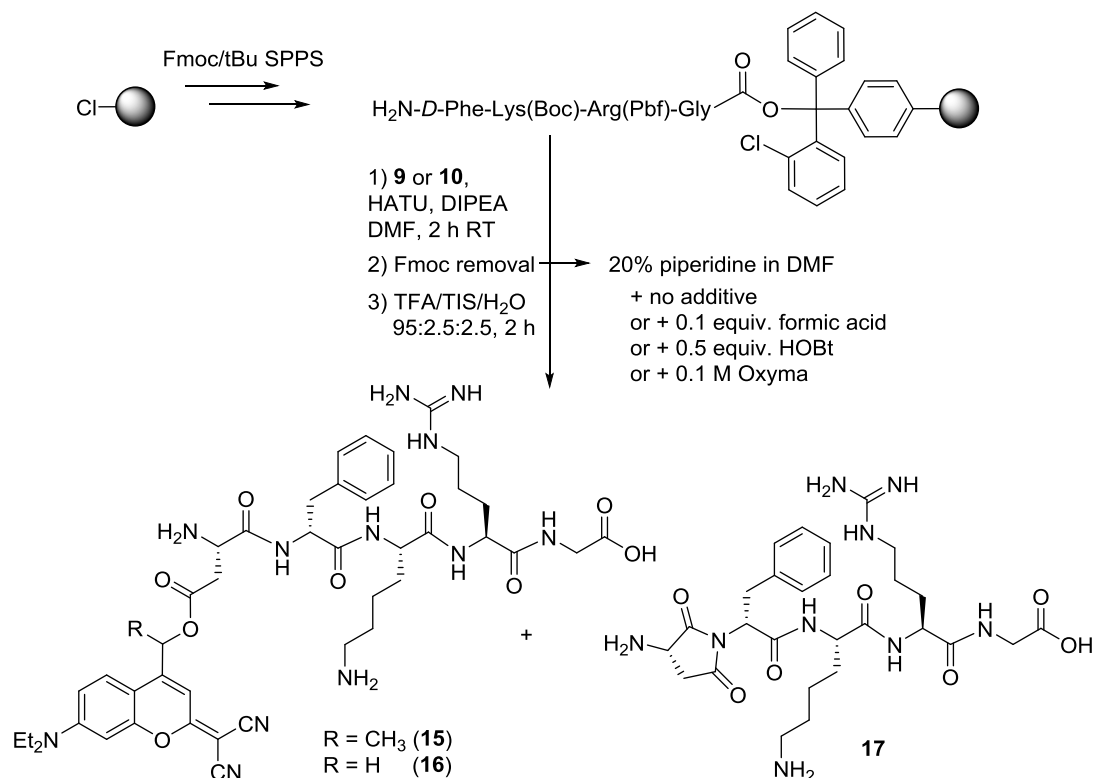


Synthesis of a dicyanocoumarin-caged cyclic RGD peptide

The next step involved the evaluation of both dicyanomethylenecoumarin derivatives (DEAdcCM and DEAdcCE) as PPGs of the side chain of Asp during the Fmoc-*t*Bu SPPS of a linear pentapeptide containing the RGD sequence (**15** and **16**, respectively; see Scheme 3). First, compounds **7** and **8** were reacted with HCl in dioxane for 15 h at 50°C to remove the *tert*-butyl group, affording the corresponding caged Asp monomers **9** and **10**, respectively (Scheme 1) suitable for the assembly of the peptide. As shown in Scheme 3, the assembly of the linear tetrapeptide was carried out on 2-chlorotrityl chloride resin using DIPC and HOAt. After incorporation of both Asp monomers (**9** or **10**) and Fmoc removal using standard conditions (20% piperidine in DMF), an acidic treatment was carried out to check the quality of the crude peptide. To our surprise, HPLC-ESI MS analysis (Figures S13 and S14 in the Supporting Information) revealed that protection of Asp with both dicyanocoumarin derivatives promotes the formation of an aspartimide side product (**17**, Scheme 3). In fact, the use of DEAdcCM monomer (**10**) did not afford the expected peptide (**16**) after standard piperidine treatment but the corresponding aspartimide derivative as a major product (Table S1 in the Supporting Information). By contrast, this undesired cyclization was substantially reduced with monomer **9**, which facilitated peptide **15** to be obtained in a 1:1 ratio with respect **17**. Aspartimide formation is well known to occur during the piperidine-catalyzed Fmoc removal of peptides containing Asp and it is very dependent on several factors including the side chain protecting group of this amino acid and its neighboring residue¹⁹ (*D*-amino acids are known to increase aspartimide

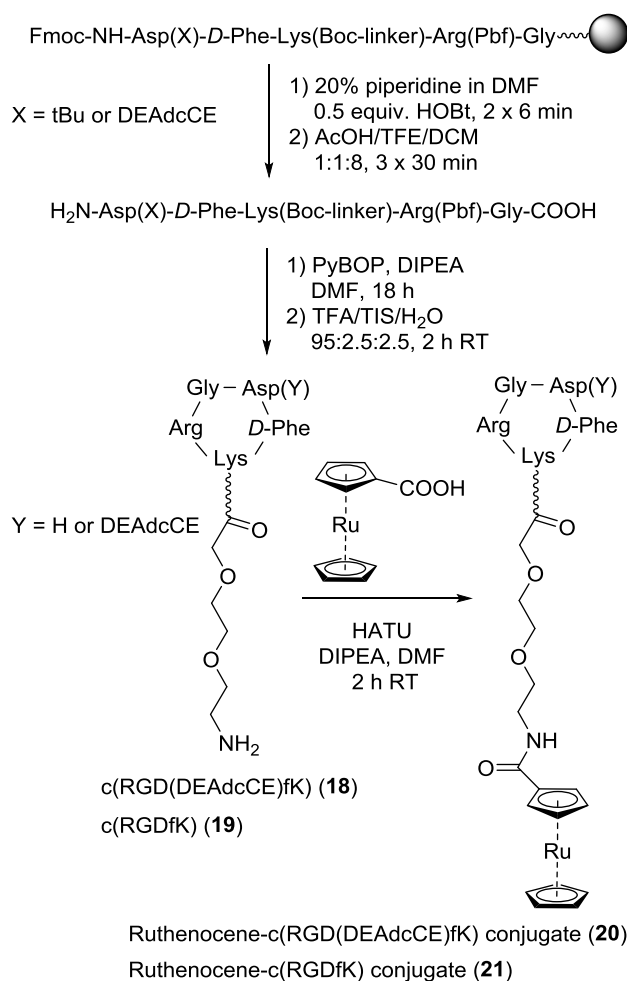
formation and in our case *D*-Phe is adjacent to the dicyanocoumarin-esterified Asp). Since the addition of organic acids to the standard piperidine-based Fmoc deprotection cocktail has been described to reduce the formation of aspartimide side products, we evaluated the use of three additives.²⁰ As shown in Figures S13 and S14 and in Table S1, HOBT and Oxyma were very effective in reducing this side reaction, particularly when the sterically-shielded DEAdcCE monomer (**9**) was used. However, the level of aspartimide was still very high with DEAdcCM monomer (**10**) under the optimal conditions for **9**. The overall results confirm that the steric hindrance provided by the methyl group of DEAdcCE around the β -carboxyl ester in combination with HOBT or Oxyma additives during Fmoc-removal represents the best choice to minimize the nucleophilic attack of the amidate anion at the carbonyl group and for instance to reduce aspartimide formation.

Scheme 3. Evaluation of aspartimide formation (compound **17**) during Fmoc-*t*Bu SPPS of the linear peptide H-Asp(DEAdcCM or DEAdcCE)-*D*-Phe-Lys-Arg-Gly-OH (**15** or **16**) by using dicyanocoumarin-protected Asp monomers (**9** or **10**, respectively) together with different Fmoc-removal conditions.



Taking into account the synthetic problems encountered with DEAdcCM monomer (**10**) together with its slow photodeprotection rate with green light, we selected DEAdcCE monomer (**9**) to synthesize the target caged cyclic RGD peptide, c(RGD(DEAdcCE)fK) (**18**). As shown in Scheme 4, a Lys building block incorporating a short Boc-protected polyethyleneglycol spacer at the ϵ -NH₂ was used during the assembly of the linear pentapeptide. After cleavage under mild acidic conditions and overnight cyclization with PyBOP, the protected peptide, c[-Arg-(Pbf)-Gly-Asp(DEAdcCE)-D-Phe-Lys(Boc-linker)-] was obtained. Finally, the remaining side chain protecting groups (Boc and Pbf) were eliminated by acidic treatment. Peptide **18** was purified by reversed-phase HPLC and characterized by HR ESI-MS (see Figures S15 and S16 in the Supporting Information). Similarly, the non-caged peptide (**19**) was synthesized as a control.^{14e}

Scheme 4. Synthesis of the DEAdcCE-caged cyclic RGD peptide (**18**) and its ruthenocenoyl conjugate (**20**).



Synthesis and photochemical properties of a conjugate between ruthenocene and the dicyanocoumarin-caged cyclic RGD peptide

Having at hand peptide **18**, we conjugated ruthenocene²¹ as a metallodrug model cargo to evaluate the compatibility of a metal complex with uncaging conditions. As shown in Scheme 4, ruthenocene carboxylic acid was attached to **18** by using HATU and DIPEA. Analysis by HPLC-ESI MS showed a main peak (Figure S17), which was isolated and characterized as the expected ruthenocene conjugate (**20**). Similarly, the control ruthenocene-RGD conjugate (**21**) was obtained by using peptide **19** (Figure S19). After purification by semipreparative HPLC and lyophilization, the trifluoroacetate salts of **20** (overall yield from **18**: 46%) and **21** (overall yield from **19**: 30%) were obtained as orange and white solids, respectively. In both cases, high-resolution ESI MS analysis afforded m/z values consistent with the calculated value of the charged species ($[M+H]^+$ and $[M+2H]^{2+}$) and with the appropriate isotopic mass distribution patterns of ruthenium (Figures S18 and S20).

Finally, the photoactivation of the coumarin-caged peptide (**18**) and its ruthenocene conjugate (**20**) was studied. As shown in Figure 3, both compounds strongly absorb in the visible region showing a maximum of absorption at $\lambda_{\max} = 496$ nm, which was slightly red-shifted with respect monomer **7** (492 nm). Irradiation of **18** at 505 nm caused a fast release of the free peptide **19** (90% after 10 min irradiation at 37°C in PBS buffer) and the corresponding coumarin alcohol **11** (Figure S21). By contrast, uncaging of conjugate **20** was slightly slower and required 30 min to achieve a similar percentage of deprotection (Figures 3 and S22), which could be attributed both to the different medium employed in the experiments and to the presence of the metal complex. A similar tendency was found when comparing the uncaging quantum yields of the caged peptide ($10^2\phi = 0.85$) and of the conjugate ($10^2\phi = 0.72$). Importantly, only ruthenocene-c(RGDfK) conjugate **21** was photoreleased from **20** upon green light irradiation, which indicates that uncaging conditions are completely compatible with the integrity of the bioconjugate. In addition, the stability of the ruthenocenoyl conjugate in cell culture medium (DMEM-25% FBS, 1 h 37°C; Figure S23) opens the door to using dicyanocoumarin-caged RGD peptides as drug carriers in cells overexpressing $\alpha_v\beta_3$ integrins.

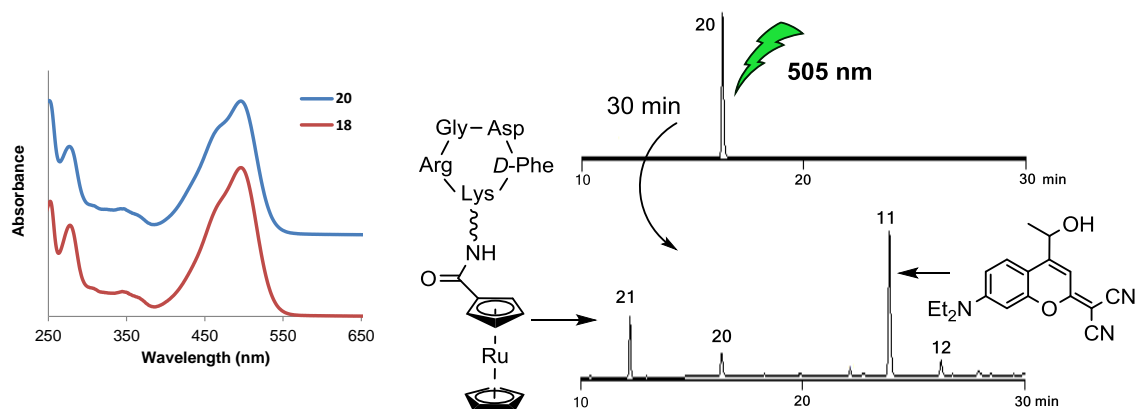


Figure 3. Left: comparison of the UV-vis spectra of peptide **18** and its ruthenocene conjugate **20**. Right: reversed-phase HPLC traces for the uncaging of conjugate **20** upon irradiation at 505 nm (37°C, PBS/ACN 8:2) at t=0 (top) and t=30 min (bottom). The structure of coumarin derivative **12** is shown in Figure S22 in the Supporting Information.

CONCLUSIONS

In summary, we have described for the first time the synthesis and photochemical characterization of a caged cyclic RGD peptide that can be efficiently photoactivated with biologically-compatible green light. This was accomplished by using a new dicyanocoumarin derivative (DEAdcCE) for the protection of the carboxyl group at the side chain of the aspartic acid residue, which was selected on the basis of Fmoc-tBu SPPS compatibility and photolysis efficiency. Indeed, the acid and basic stability of dicyanocoumarin-caged Asp monomers (**7** and **8**) was found to be substantially higher than that of the thiocoumarin precursors (**5** and **6**) and, among them, the DEAdcCE moiety was preferred over DEAdcCM due to higher uncaging efficiency and reduced aspartimide formation. Minimization of aspartimide side-reaction was accomplished by using acidic additives such as HOBT or Oxyma during the basic Fmoc-removal treatment in combination with the Fmoc-Asp(DEAdcCE)-OH monomer (**9**) in which the incorporation of a methyl group at the coumarin skeleton near the ester bond linking both moieties led to a steric shielding effect around this functionality.

On the other hand, a conjugate between the coumarin-caged cyclic RGD peptide and ruthenocene, which was selected as a metallodrug model cargo, has been synthesized and characterized. The fact that green-light triggered photoactivation can be efficiently performed both with the caged peptide (**18**) and with its ruthenocenoil bioconjugate (**21**) opens the door to exploring the use of DEAdcCE-caged peptide sequences as selective drug carriers in the context of photocontrolled targeted anticancer strategies. Work is in progress to extend this approach to other coumarin derivatives with improved red-shifted properties, particularly those removable within the optical window of the tissues, as well as to the conjugation between caged peptides and other anticancer agents, including Pt(IV) pro-drugs.

EXPERIMENTAL SECTION

Materials and Methods.

Unless otherwise stated, common chemicals and solvents including Fmoc-protected amino acids, resins and coupling reagents for solid-phase synthesis were purchased from commercial sources and used without further purification. Milli-Q water was directly obtained from a Milli-Q system equipped with a 5000-Da ultrafiltration cartridge. Aluminium plates coated with a 0.2 mm thick layer of silica gel 60 F₂₅₄ were used for thin-layer chromatography analyses (TLC), whereas column chromatography purification was carried out using silica gel 60 (230-400 mesh). Analytical reversed-phase HPLC analyses were carried out on a Jupiter Proteo column (250x4.6 mm, 4 μ m, flow rate: 1 mL/min), using linear gradients of 0.045% TFA in H₂O (solvent A) and 0.036% TFA in ACN (solvent B). In some cases, small-scale purification was carried out using the same column. Large-scale purification was carried out on a Jupiter Proteo semipreparative column (250 x 10 mm, 10 μ m, flow rate: 3 mL/min), using linear gradients of 0.1% TFA in H₂O (solvent A) and 0.1% TFA in ACN (solvent B). After several runs, pure fractions were combined and lyophilized. Electrospray ionization mass spectra (ESI-MS) were recorded on an instrument equipped with single quadrupole detector coupled to an HPLC, and high-resolution (HR) ESI-MS on LC/MSTOF instrument. NMR spectra were recorded at 25°C in a 400 MHz spectrometer using deuterated solvents. Tetramethylsilane (TMS) was used as an internal reference (0 ppm) for ¹H spectra recorded in CDCl₃ and the residual signal of the solvent (77.16 ppm) for ¹³C spectra. Chemical shifts are reported in part per million (ppm) in the δ scale, coupling constants in Hz and multiplicity as follows: s (singlet), d (doublet), t (triplet), q (quadruplet), qt (quintuplet), m (multiplet), dd (doublet of doublets), td (doublet of triplets), ddd (doublet of doublet of doublets), br (broad signal). UV-vis spectra were recorded with a UV-Vis-NIR spectrophotometer and fluorescence measurements were performed on a QuantaMaster fluorimeter. Photolysis studies were performed at 37°C in a custom-built irradiation setup from Microbeam including a cuvette, thermostated cuvette holder and a mounted high power LED of 505 nm (100 mW/cm²). In a typical experiment, the irradiation samples

contained the caged amino acids (20 μ M) in a 1:1 (v/v) mixture of Tris buffer pH 7.5 and ACN. After irradiation, the samples were analyzed by reversed-phase HPLC-ESI MS in a Jupiter Proteo C₁₈ column (250x4.6 mm, 90 Å 4 μ m, flow rate: 1 mL/min) using linear gradients of 0.1% formic acid in H₂O (A) and 0.1% formic acid in ACN (B).

Synthesis of the caged amino acid derivatives.

7-(N,N-diethylamino)-4-(1-hydroxyethyl-1-yl)-coumarin (1)^{7e}

A solution of 4-carbaldehyde-7-(N,N-diethylamino)coumarin (2.58 g, 11 mmol) in dry THF (60 mL) was cooled at -78°C using a mixture of acetone and dry ice and kept under argon atmosphere. Then, a solution of methylmagnesium chloride (6.3 mL, 3 M) in THF was added dropwise and the reaction mixture was stirred for 2 h at -78°C in the dark. After that, a second portion of methylmagnesium chloride (3.0 mL) was added. After stirring 2 additional hours at -78°C in the dark, a saturated aqueous solution of ammonium chloride (50 mL) was added and the reaction mixture was allowed to reach room temperature. The mixture was extracted with ethyl acetate (3 x 50 mL). The combined organic layers were dried over Na₂SO₄, filtered and the solvent was removed under reduced pressure. The red residue was purified by column chromatography (silica gel, 0-3.5% MeOH in DCM). The appropriate fractions were collected and the solvents were removed to give a 1.94 g (71% yield) of a yellow solid. TLC: R_f (5% MeOH in DCM) 0.31. ¹H NMR (400 MHz, CDCl₃) δ (ppm): 7.43 (1H, d, J= 9.2 Hz), 6.57 (1H, dd, J= 9.2 Hz, J= 2.6 Hz), 6.50 (1H, d, J= 2.6 Hz), 6.27 (1H, br s), 5.15 (1H, m), 3.41 (4H, q, J= 7.0Hz), 2.18 (1H, br s), 1.57 (3H, d, J= 6.8 Hz), 1.21 (6H, t, J= 7.0 Hz). ESI-MS, positive mode: *m/z* 261.55 (calcd mass for C₁₅H₂₀NO₃ [M+H]⁺: 262.14).

7-(N,N-Diethylamino)-4-hydroxymethylcoumarin (2)^{7e}

4-carbaldehyde-7-(N,N-diethylamino)coumarin (3.71 g, 15.1 mmol) and sodium borohydride (0.57 g, 15.1 mmol) were stirred at room temperature for 4 h in ethanol (300 mL) protected from light. After addition of 1 M HCl (80 mL) and dilution with water (50 mL), the red solution was extracted with DCM (3 x 50 mL). The combined organic layers were washed with water (50 mL), dried over anhydrous MgSO₄ and filtered. After removal of the solvent under reduced pressure, a red solid was obtained (3.31 g, yield 90%) and used without further purification in

the next step. TLC: R_f (5% MeOH in DCM) 0.25. ^1H NMR (400 MHz, CDCl_3) δ (ppm): 7.31 (1H, d, $J=9.2$ Hz), 6.57 (1H, dd, $J=9.2$ Hz, $J=2.8$ Hz), 6.49 (1H, d, $J=2.8$ Hz), 6.26 (1H, s, H_3), 4.83 (2H, s), 3.40 (4H, q, $J=7.2$ Hz), 1.20 (6H, t, $J=7.2$ Hz). ESI-MS, positive mode: m/z 247.88 (calcd mass for $\text{C}_{14}\text{H}_{18}\text{NO}_3$ $[\text{M}+\text{H}]^+$: 248.13).

Fmoc-Asp(DEACE)-O^tBu (3)^{7e}

Fmoc-Asp-O^tBu (2.52 g, 6.12 mmol), 1-ethyl-3-(3-dimethylaminopropyl)carbodiimide hydrochloride (1.39 g, 7.25 mmol) and DMAP (38 mg, 0.31 mmol) were dissolved in dry DCM (50 mL). A solution of **1** (1.44 g, 5.56 mmol) in dry DCM (50 mL) was added and the reaction mixture was stirred at room temperature in the dark under argon atmosphere for 4 h. The solvent was removed in vacuum and the crude material was purified via column chromatography (silica gel, 0-1.5% methanol in DCM) to obtain 1.42 g (57 % yield) of a yellow crystalline solid. TLC: R_f (5% MeOH in CH_2Cl_2) 0.68. ^1H NMR (400 MHz, CDCl_3) δ (ppm): 7.75 (2H, t, $J=6.8$ Hz), 7.58 (2H, t, $J=6.8$ Hz), 7.39 (3H, q, $J=7.2$ Hz), 7.31 (2H, t, $J=7.2$ Hz), 6.57 (1H, ddd, $J=8.8$ Hz, $J=6$ Hz, $J=2.4$ Hz), 6.50 (1H, dd, $J=5.6$ Hz, $J=2.4$ Hz), 6.12 (1H, d, $J=4$ Hz), 6.06 (1H, m), 5.75 (1H, m), 4.55 (1H, m), 4.35 (2H, m), 4.22 (1H, q, $J=6.8$ Hz), 3.39 (4H, q, $J=7.2$ Hz), 3.02 (2H, m), 1.60 (3H, d, $J=6.4$ Hz), 1.56 (1H, s), 1.48 (4H, s), 1.40 (4H, s), 1.19 (6H, dt, $J=7.2$ Hz). ^{13}C NMR (100 MHz, CDCl_3) δ (ppm): 170.1, 169.9, 169.5, 169.3, 162.0, 161.9, 156.6, 155.9, 155.1, 154.8, 150.6, 143.9, 143.8, 143.7, 141.2, 127.7, 127.1, 125.2, 124.8, 124.6, 120.0, 119.9, 108.7, 105.5, 105.1, 104.9, 98.0, 83.0, 82.9, 68.4, 68.2, 67.3, 50.9, 50.8, 47.1, 44.7, 36.9, 27.9, 27.8, 20.9, 12.4. ESI-MS, positive mode: m/z 654.9 (calcd mass for $\text{C}_{38}\text{H}_{42}\text{N}_2\text{O}_8$ $[\text{M}+\text{H}]^+$: 654.76).

Fmoc-Asp(DEACM)-O^tBu (4)^{7e}

Fmoc-Asp-O^tBu (1.83 g, 4.45 mmol), 1-ethyl-3-(3-dimethylaminopropyl)carbodiimide hydrochloride (1.01 g, 5.27 mmol) and DMAP (25 mg, 0.20 mmol) were dissolved in dry DCM (50 mL). After addition of a solution of **2** (1.01 g, 4.09 mmol) in dry DCM (50 mL), the reaction mixture was stirred at room temperature in the dark under argon atmosphere for 4 h. The solvent was removed under vacuum and the crude material was purified via column chromatography (silica gel, 0-3% MeOH in DCM) to obtain 1.37 g (53% yield) of a yellow

crystalline solid. TLC: R_f (5% MeOH in DCM) 0.74. ^1H NMR (400 MHz, CDCl_3) δ (ppm): 7.76 (2H, d, $J=7.7$ Hz), 7.60 (2H, d, $J=7.2$ Hz), 7.39 (2H, t, $J=7.2$ Hz), 7.31 (3H, m), 6.56 (1H, m), 6.51 (1H, m), 6.12 (1H, s), 5.75 (1H, d, $J=7.6$ Hz), 5.24 (2H, m), 4.58 (1H, m), 4.38 (2H, m), 4.23 (1H, t, $J=7.2$ Hz), 3.40 (4H, q, $J=7.2$ Hz), 3.04 (2H, m), 1.46 (9H, s), 1.19 (6H, t, $J=7.2$ Hz). ^{13}C NMR (100 MHz, CDCl_3) δ (ppm): 170.3, 169.4, 161.7, 156.3, 155.9, 150.7, 148.8, 143.8, 141.3, 127.7, 127.1, 125.2, 124.4, 120.0, 108.7, 106.8, 105.9, 97.9, 83.1, 67.3, 61.9, 50.9, 47.1, 44.8, 36.8, 27.9, 12.4. ESI-MS, positive mode: m/z 640.95 (calcd mass for $\text{C}_{37}\text{H}_{41}\text{N}_2\text{O}_8$ $[\text{M}+\text{H}]^+$: 641.29).

Fmoc-Asp(DEATCE)-O^tBu (5)

Lawesson's reagent (0.41 g, 1.01 mmol) was added to a solution of Fmoc-Asp(DEACE)-O^tBu (**3**, 1.10, 1.68 mmol) in toluene (40 mL). After stirring overnight at 70°C under an argon atmosphere and protected from light, the solvent was evaporated under reduced pressure and the resulting orange crude solid was purified via column chromatography (silica gel, 0-1% MeOH in DCM) to obtain 0.91 g (81% yield) of dark orange solid; mp 95-97 °C. TLC: R_f (2% MeOH in DCM) 0.71. ^1H NMR (400 MHz, CDCl_3) δ (ppm): 7.75 (2H, m), 7.58 (2H, m), 7.40 (3H, m), 7.31 (2H, m), 7.04 (1H, d, $J=6$ Hz), 6.65 (2H, m), 6.08 (1H, m), 5.74 (1H, t, $J=8$ Hz), 4.55 (1H, m), 4.37 (2H, m), 4.23 (1H, m), 3.41 (4H, m), 3.10-2.92 (2H, m), 1.59 (4H, m), 1.48 (4H, s), 1.40 (4H, s), 1.21 (6H, m). ^{13}C NMR (100 MHz, CDCl_3) δ (ppm): 197.3, 197.2, 170.1, 170.0, 169.5, 169.3, 159.4, 155.9, 150.9, 147.3, 147.0, 143.9, 143.8, 141.3, 127.7, 127.1, 125.2, 124.8, 124.7, 120.0, 119.3, 119.1, 110.4, 107.8, 97.7, 83.0, 82.9, 68.1, 67.9, 67.3, 67.2, 53.4, 50.8, 50.8, 47.1, 44.9, 37.0, 36.9, 27.9, 27.8, 20.9, 20.8, 12.4. HR ESI-MS, positive mode: m/z 671.2777 (calcd mass for $\text{C}_{38}\text{H}_{43}\text{N}_2\text{O}_7\text{S}$ $[\text{M}+\text{H}]^+$: 671.2791). Analytical RP-HPLC (0 to 100% B in 30 min, 10 min isocratic 100% B; A: 0.1 % formic acid in H_2O , B: 0.1% formic acid in ACN; $R_t = 32$ min).

Fmoc-Asp(DEATCM)-O^tBu (6)

Lawesson's reagent (1.18 g, 2.92 mmol) was added to Fmoc-Asp(DEACM)-O^tBu (**4**, 1 g, 1.56 mmol) in toluene (50 mL). The mixture was stirred overnight at 70°C under an argon atmosphere and protected from light. After that, the solvent was evaporated under vacuum and

the resulting crude was purified via column chromatography (silica gel, 0-1% MeOH in DCM) to give 0.82 g (80% yield) of a dark orange solid; mp 91-94 °C. TLC: R_f (2% MeOH in DCM) 0.71. ^1H NMR (400 MHz, CDCl_3) δ (ppm): 7.76 (2H, d, $J=7.2$ Hz), 7.60 (2H, dm $J=7.2$ Hz), 7.40 (2H, t, $J=7.6$ Hz), 7.31 (3H, q, $J=6.0$ Hz), 7.03 (1H, s), 6.66 (1H, d, $J=2.4$ Hz), 6.63 (1H, dd, $J=9.2$ Hz, $J=2.4$ Hz), 5.74 (1H, d, $J=8.0$ Hz), 5.20 (2H, m), 4.58 (1H, m), 4.39 (2H, m), 4.23 (1H, t, $J=7.2$ Hz), 3.41 (4H, q, $J=7.2$ Hz), 3.05 (2H, m), 1.47 (9H, s), 1.20 (6H, t, $J=7.2$ Hz). ^{13}C NMR (100 MHz, CDCl_3) δ (ppm): 197.0, 170.3, 169.3, 159.1, 155.9, 151.0, 143.8, 141.3, 141.1, 127.7, 127.1, 125.2, 124.5, 121.0, 120.0, 110.3, 108.2, 97.5, 83.1, 67.3, 61.6, 53.4, 50.9, 47.1, 44.9, 36.8, 27.9, 12.4. HR ESI-MS, positive mode: m/z 657.2623 (calcd mass for $\text{C}_{37}\text{H}_{41}\text{N}_2\text{O}_7\text{S}$ $[\text{M}+\text{H}]^+$: 657.2634). Analytical RP-HPLC (30 to 100% B in 30 min; A: 0.1 % formic acid in H_2O , B: 0.1% formic acid in ACN; $R_t = 25.5$ min).

Fmoc-Asp(DEAdcCE)-O'Bu (7)

Silver nitrate (580 mg, 3.42 mmol) was added to a solution of Fmoc-Asp(DEATCE)-OtBu (**5**, 920 mg, 1.37 mmol), malononitrile (453 mg, 6.85 mmol) and triethylamine (670 μL , 4.79 mmol) in dry ACN (80 mL) under an argon atmosphere. The reaction mixture was stirred for 3 h in the dark at room temperature and then concentrated under reduced pressure. The crude was purified by column chromatography (silica gel, 0-0.6% MeOH in DCM) to give 780 mg (81 % yield) of a dark orange solid; mp 110-113 °C. TLC: R_f (2% MeOH in DCM) 0.65 ^1H NMR (400 MHz, CDCl_3) δ (ppm): 7.75 (2H, m), 7.57-7.53 (2H, m), 7.45-7.27 (5H, m), 6.70 (1H, m), 6.64 (1H, m), 6.57-6.52 (1H, m), 6.07 (1H, m), 5.73 (1H, br t), 4.56 (1H, m), 4.35 (2H, m), 4.18 (1H, m), 3.46-3.36 (4H, m), 3.02 (2H, m), 1.60 (3H, m), 1.49 (5H, s), 1.40 (4H, s), 1.21 (6H, m). ^{13}C NMR (100 MHz, CDCl_3) δ (ppm): 171.9, 170.0, 169.4, 169.2, 155.9, 155.8, 155.3, 151.8, 151.6, 151.5, 151.3, 143.8, 143.7, 141.2, 127.4, 127.0, 125.1, 119.9, 114.6, 113.8, 110.7, 110.6, 106.5, 104.8, 104.4, 97.5, 82.9, 68.3, 67.2, 55.4, 55.3, 50.9, 47.1, 44.9, 36.9, 29.7, 27.9, 27.8, 21.0, 12.4. HR ESI-MS, positive mode: m/z 703.3114 (calcd mass for $\text{C}_{41}\text{H}_{43}\text{N}_4\text{O}_7$ $[\text{M}+\text{H}]^+$: 703.3132). Analytical RP-HPLC (30 to 100% B in 30 min; A: 0.1 % formic acid in H_2O , B: 0.1% formic acid in ACN; $R_t = 25.7$ and 25.8 min).

Fmoc-Asp(DEAdcCE)-O'Bu (8)

Silver nitrate (323 mg, 1.90 mmol) was added to a solution of Fmoc-Asp(DEATCM)-OtBu (**6**, 500 mg, 0.76 mmol), malononitrile (352 mg, 5.33 mmol) and triethylamine (370 μ L, 2.67 mmol) in dry ACN (40 mL) under an argon atmosphere. The reaction mixture was stirred for 3 h in the dark at room temperature and then concentrated under reduced pressure. The crude was purified by column chromatography (silica gel, 0-0.8% MeOH in DCM) to give 337 mg (65 % yield) of a dark orange solid; mp 108-110 °C. TLC: R_f (2% MeOH in DCM) 0.74. ^1H NMR (400 MHz, CDCl_3) δ (ppm): 7.75 (2H, d, $J=7.5$ Hz), 7.58 (2H, d, $J=7.4$ Hz), 7.39 (2H, t, $J=7.4$ Hz), 7.30 (3H, m), 6.73 (1H, s), 6.62 (1H, dd, $J=9$ Hz, $J=2.4$ Hz), 6.55 (1H, d, $J=2.4$ Hz), 5.75 (1H, d, $J=7.6$ Hz), 5.23 (2H, q, $J=15$ Hz), 4.57 (1H, m), 4.37 (2H, m), 4.20 (1H, t, $J=7.1$ Hz), 3.41 (4H, q, $J=7.2$ Hz), 3.05 (2H, m), 1.47 (9H, s), 1.21 (6H, t, $J=7.2$ Hz). ^{13}C NMR (100 MHz, CDCl_3) δ (ppm): 171.6, 170.2, 169.3, 155.9, 155.0, 151.7, 145.2, 143.7, 141.3, 127.7, 127.1, 125.1, 125.0, 120.0, 114.4, 113.7, 110.6, 107.0, 106.5, 97.4, 83.1, 67.2, 61.7, 55.9, 51.0, 47.1, 44.9, 36.9, 27.9, 12.4. HR ESI-MS, positive mode: m/z 689.2977 (calcd mass for $\text{C}_{40}\text{H}_{41}\text{N}_4\text{O}_7$ $[\text{M}+\text{H}]^+$: 689.2975). Analytical RP-HPLC (30 to 100% B in 30 min; A: 0.1 % formic acid in H_2O , B: 0.1% formic acid in ACN; $R_t = 24.5$ min).

Fmoc-Asp(DEAdcCE)-OH (9)

A solution of HCl in 1,4-dioxane (20 mL, 100 mmol) was added to a Fmoc-Asp(DEAdcCE)-OtBu (**7**, 600 mg, 0.85 mmol). The reaction mixture was stirred in the dark at 50°C during 15 h and then concentrated under reduced pressure. The compound was used directly in the assembly of the caged peptide. ^1H NMR (400 MHz, CDCl_3) δ (ppm): 7.75 (2H, d, $J=7.2$ Hz), 7.57-7.53 (2H, m), 7.38 (3H, t, $J=7.6$ Hz), 7.30-7.27 (2H, m), 6.66-6.64 (2H, m), 6.56-6.53 (1H, m), 6.12-6.05 (1H, m), 5.82 (1H, m), 4.75-4.70 (1H, m), 4.41-4.35 (2H, m), 4.19 (1H, m), 3.66-3.62 (4H, m), 3.11 (2H, m), 1.59 (3H, m), 1.22 (6H, m). ^{13}C NMR (100 MHz, CDCl_3) δ (ppm): 172.1, 169.6, 169.1, 155.8, 155.7, 155.2, 151.7, 151.5, 143.5, 143.4, 141.1, 127.6, 126.9, 124.9, 119.8, 115.6, 113.5, 110.7, 106.3, 104.1, 103.9, 97.4, 72.0, 71.0, 67.2, 61.5, 54.8, 49.9, 46.8, 44.8, 42.7, 36.7, 29.5, 21.0, 12.6. HR ESI-MS, positive mode: m/z 647.2518 (calcd mass for $\text{C}_{37}\text{H}_{35}\text{N}_4\text{O}_7$ $[\text{M}+\text{H}]^+$: 647.2506). Analytical RP-HPLC (30 to 100% B in 30 min; A: 0.1 % formic acid in H_2O , B: 0.1% formic acid in ACN; $R_t = 23.5$ min).

Fmoc-Asp(DEAdcCE)-OH (10)

A solution of HCl in 1,4-dioxane (5 mL, 25 mmol) was added to a Fmoc-Asp(DEAdcCM)-OtBu (**8**, 30mg, 0.04 mmol). The reaction mixture was stirred in the dark at 50°C during 15 h and then concentrated under reduced pressure. The compound was used directly in the assembly of the caged peptide. ¹H NMR (400 MHz, CDCl₃) δ (ppm): 7.75 (2H, d, J= 7.2 Hz), 7.58 (2H, m), 7.39 (2H, t, J= 7.2 Hz), 7.30 (3H, m), 6.70-6.61 (3H, m), 5.88 (1H, m), 5.29 (2H, m), 4.76 (1H, m), 4.40 (2H, m), 4.21 (1H, m), 3.65 (4H, q, J= 7.2 Hz), 3.18 (2H, m), 1.21 (6H, m). ¹³C NMR (100 MHz, CDCl₃) δ (ppm): 172.4, 172.17, 170.1, 156.1, 155.0, 151.7, 146.0, 143.8, 141.4, 127.9, 127.3, 125.2, 125.0, 120.1, 115.8, 113.6, 111.2, 107.1, 105.7, 97.7, 72.4, 71.3, 67.5, 61.8, 55.3, 50.3, 47.2, 45.3, 43.0, 36.9, 12.6. HR ESI-MS, positive mode: *m/z* 633.2334 (calcd mass for C₃₆H₃₃N₄O₇ [M+H]⁺: 633.2349). Analytical RP-HPLC (30 to 100% B in 30 min; A: 0.1 % formic acid in H₂O, B: 0.1% formic acid in ACN; R_t = 22.7 min).

Synthesis DEAdcCE-caged RGD peptide (18)

Solid-phase peptide syntheses were performed manually in a polypropylene syringe fitted with a polyethylene disc. Standard Fmoc/tBu chemistry was used with 2-chlorotrityl chloride resin (f = 1.5 mmol/g, 100-200 mesh). The following protecting groups were used for the protection of trifunctional amino acids: Boc (*N*^ε-*tert*-butoxycarbonyl, Lys), Pbf (*N*^G-2,2,4,6,7-pentamethyldihydrobenzofuran-5-sulfonyl, Arg) and ^tBu (*O*-*tert*-butyl, Asp). Fmoc-Asp(DEAdcCE)-OH (**9**) or Fmoc-Asp(DEAdcCM)-OH (**10**) were used for the synthesis of caged peptides, and Fmoc-Lys(Boc-AEEA)-OH (Boc-AEEA = *N*^ε-(2-(2-(2-(*tert*-butyloxycarbonyl)aminoethoxy)ethoxy)acetyl) was used as spacer. First, the resin was washed with neutral DCM (2 x 5 min and 1 x 30 min) and the loading was reduced to *ca* 1 mmol/g by incorporation of Fmoc-Gly-OH (0.7 mol equiv.) in the presence of DIPEA (5 mol equiv.) in anhydrous DCM for 40 min. After capping with MeOH (1 x 10 min), the following Fmoc-protected amino acids (3 mol equiv.) were incorporated with DIPC (3 mol equiv.) and HOAt (3 mol equiv.) in anhydrous DMF for 2 h. The coupling efficiency was assessed by the ninhydrin test. Fmoc protecting groups were removed with 20% piperidine in DMF (2 x 10 min) in each synthesis cycle except when using DEAdcCE or DEAdcCM protection for Asp, which required

the use of an acidic additive (0.5 equiv. HOBt relative to piperidine). After removal of the final *N*-terminal Fmoc group, linear peptides were released from the support by treatment with AcOH/TFE/DCM 1:1:8 (v/v/v) (3 x 30 min). The collected filtrates were evaporated *in vacuo*, and several co-evaporations with toluene (4 x 25 mL) were carried out to remove completely acetic acid. The resulting residue was dissolved in the minimum amount of DCM and poured onto cold diethyl ether to precipitate the fully protected linear peptide. The crude was triturated and washed three times with ether. Cyclization was carried out in DMF (*ca* 1 mL/ mg crude peptide) at pH 8-9 (adjusted with DIPEA) by using PyBOP (1 mol equiv.). After it was stirred for 18 h at room temperature, the reaction mixture was evaporated *in vacuo* and diethyl ether was used to precipitate the peptides. Finally, side-chain deprotection was performed with TFA/TIS/H₂O 95:2.5:2.5 for 2 h at room temperature. After evaporation under reduced pressure, the crude peptide was triturated and washed three times with cold diethyl ether. After purification by semipreparative HPLC (gradient from 0 to 100% B in 30 min, A: 0.1 % TFA in H₂O; B: 0.1% TFA in ACN flow rate: 3 mL/min), the trifluoroacetate salt of the peptide was obtained.

***c(RGD(DEAdcCE)fK)* (18)**. Overall yield (synthesis + purification): 22 mg, 5%. Characterization: Analytical RP-HPLC (0 to 100% B in 30 min; A: 0.1 % formic acid in H₂O, B: 0.1% formic acid in ACN): R_t = 12.7 min; HR ESI MS, positive mode: *m/z* 1040.5302 (calcd mass for C₅₁H₇₀N₁₃O₁₁ [M+H]⁺: 1040.5318), *m/z* 520.7698 (calcd mass for C₅₁H₇₁N₁₃O₁₁ [M+2H]²⁺: 520.7698).

Synthesis of ruthenocenoyl-peptide conjugates (20 and 21)

Ruthenocene-c(RGD(DEAdcCE)fK) conjugate (20). To a solution of ruthenocene carboxylic acid (0.35 mg, 1.3 mol equiv.) and HATU (0.51 mg, 1.05 mol equiv.) in anhydrous DMF (0.2 mL), DIPEA (2 μL, 10 mol equiv.) was added. After stirring for 5 min at room temperature, the reaction mixture was added to peptide **18** (1.0 mg, 0.91 μmol) previously dissolved in anhydrous DMF (0.2 mL) and DIPEA (1 μL, 5 mol equiv.). After stirring for 2 h at room temperature and protected from light, the solvent was evaporated *in vacuo* and the conjugate was purified by semipreparative HPLC (gradient from 50 to 100% B in 30 min, flow rate: 3

mL/min, $R_t = 9.5$ min). Overall yield (synthesis + purification): 0.57 mg of a orange solid, 46%. Characterization: $R_t = 16.4$ min (analytical gradient: 0 to 100 % in 30 min; A: 0.1 % formic acid in H_2O , B: 0.1% formic acid in ACN); HR ESI MS, positive mode: m/z 1298.4928 (calcd mass for $C_{62}H_{78}N_{13}O_{12}Ru$ $[M+H]^+$: 1298.4936).

-Ruthenocene-c(RGDfK) conjugate (21). To a solution of ruthenocene carboxylic acid (0.48 mg, 1.3 mol equiv.) and HATU (0.72 mg, 1.05 mol equiv.) in anhydrous DMF (0.2 mL), DIPEA (2.4 μ L, 10 mol equiv.) was added. After stirring for 5 min at room temperature, the reaction mixture was added to peptide **19** (1 mg, 1.33 μ mol) previously dissolved in anhydrous DMF (0.2 mL) and DIPEA (1.2 μ L, 5 mol equiv.). After stirring for 2 h at room temperature, the solvent was evaporated *in vacuo* and the conjugate was purified by semipreparative HPLC (gradient from 0 to 100% B in 30 min, flow rate: 3 mL/min, $R_t = 14.9$ min). Overall yield (synthesis + purification): 0.42 mg of a white solid, 30%. Characterization: $R_t = 12.2$ min (analytical gradient: 0 to 100 % in 30 min; A: 0.1 % formic acid in H_2O , B: 0.1% formic acid in ACN); HR ESI MS, positive mode: m/z 1007.3561 (calcd mass for $C_{44}H_{61}N_{10}O_{11}Ru$ $[M+H]^+$: 1007.3565).

ASSOCIATED CONTENT

Supporting Information

Characterization data (HPLC traces, NMR, MS, UV-vis and fluorescence) of the compounds.

This material is available free of charge via the Internet at <http://pubs.acs.org>.

AUTHOR INFORMATION

Corresponding Author

*E-mail: vmarchan@ub.edu.

ACKNOWLEDGEMENTS

This work was supported by funds from the Spanish grants CTQ2014-52658-R and CSD2009-00080, and the Generalitat de Catalunya (2014SGR187 and XRB). The authors acknowledge

helpful assistance of Dr. Irene Fernández and Laura Ortiz (MS), and Dr. Francisco Cárdenas (NMR) from CCI-TUB. A.G. was a recipient fellow of the University of Barcelona.

REFERENCES

- (1) (a) Briek, C.; Rohrbach, F.; Gottschalk, A.; Mayer, G.; Heckel, A. *Angew. Chem. Int. Ed.* **2012**, *51*, 8446-8476. (b) Hansen, M. J.; Velema, W. A.; Lerch, M. M.; Szymanski, W.; Feringa, B. L. *Chem. Soc. Rev.* **2015**, *44*, 3358-3377. (c) Velema, W. A.; Szymanski, W.; Feringa, B. L. *J. Am. Chem. Soc.* **2014**, *136*, 2178-2791. (d) Szymański, W.; Beierle, J. M. Kistemaker, H. A. V.; Velema, W. A.; Feringa, B. L. *Chem. Rev.* **2013**, *113*, 6114–6178.
- (2) (a) Lee, H.-M.; Larson, D. R.; Lawrence, D. S. *ACS Chem. Biol.* **2009**, *4*, 409-427. (b) Deiters, A. *ChemBioChem.* **2010**, *11*, 47-53.
- (3) Klan, P.; Solomek, T.; Bochet, C. G.; Blanc, A.; Givens, R.; Rubina, M.; Popik, V.; Kostikov, A.; Wirz, J. *Chem. Rev.* **2013**, *113*, 119-191.
- (4) (a) Mayer, G.; Heckel, A. *Angew. Chem. Int. Ed.* **2006**, *45*, 4900-4921. (b) Noguchi, M.; Skwarczynski, M.; Prakash, H.; Hirota, S.; Kimura, T.; Hayashia, Y.; Kisoa, Y. *Bioorg. Med. Chem.* **2008**, *16*, 5389–5397. (c) Schimer, J.; Pávová, M.; Anders, M.; Pachel, P.; Šácha, P.; Cígler, P.; Weber, J.; Majer, P.; Řezáčová, P.; Kräusslich, H.-G.; Müller, B.; Konvalinka, J. *Nature Commun.* **2015**, *6*, 6461-6468. (d) Velema, W. A.; van der Berg, J. P.; Szymanski, W.; Driessen, A. J. M.; Feringa, B. L. *ACS Chem. Biol.* **2014**, *9*, 1969-1974. (e) Olson, J. P.; Kwon, H.-B.; Takasaki, K. T.; Chiu, C. Q.; Higley, M. J.; Sabatini, B. L.; Ellis-Davies, G. C. R. *J. Am. Chem. Soc.* **2013**, *135*, 5954-5957. (f) Furuta, T.; Wang, S. S.-H.; Dantzker, J. L.; Dore, T. M.; Bybee, W. J.; Callaway, E. M.; Denk, W.; Tsien, R. Y. *Proc. Natl. Acad. Sci. USA* **1999**, *96*, 1193-1200. (g) Schönleber, R. O.; Bendig, J.; Hagen, V.; Giese, B. *Bioorg. Med. Chem.* **2002**, *10*, 97-101 (h) Agarwal, H. K.; Janicek, R.; Chi, S.-H.; Perry, J. W.; Niggli, E.; Ellis-Davies, G. C. R. *J. Am. Chem. Soc.* **2016**, *138*, 3687-3693.
- (5) (a) Azagarsamy, M. A.; Anseth, K. S. *Angew. Chem., Int. Ed.* **2013**, *52*, 13803-13807. (b) A. Gautier; Gauron, C.; Volovitch, M.; Bensimon, D.; Jullien, L.; Vríz, S. *Nat. Chem. Biol.* **2014**, *10*, 533-541.

- (6) (a) Steinert, H. S.; Schäfe, F.; Jonker, H. R.; Heckel, A.; Schwalbe, H. *Angew. Chem., Int. Ed.* **2014**, *53*, 1072-1075. (b) Meyer, A.; Mokhir, A. *Angew. Chem., Int. Ed.* **2014**, *53*, 12840-12843. (c) Rodrigues-Correia, A.; Knapp-Bühle, D.; Engels, J. W.; Heckel, A. *Org. Lett.* **2014**, *16*, 5128-5131. (d) Hemphill, J.; Liu, Q.; Uprety, R.; Samanta, S.; Tsang, M.; Juliano, R. L.; Deiters, A. *J. Am. Chem. Soc.* **2015**, *137*, 3656-3662.
- (7) (a) Bourgault, S.; Létourneau, M.; Fournier, A. *Peptides* **2005**, *26*, 1475-1480. (b) Bourgault, S.; Létourneau, M.; Fournier, A. *Peptides* **2007**, *28*, 1074-1082. (c) Petersen, S.; Alonso, J. M.; Specht, A.; Duodu, P.; Goeldner, M.; del Campo, A. *Angew. Chem. Int. Ed.* **2008**, *47*, 3192-3195. (d) Wirkner, M.; Weis, S.; San Miguel, V.; Alvarez, M.; Gropeanu, R. A.; Salierno, M.; Sartoris, A.; Unger, R. E.; Kirkpatrick, C. J.; del Campo, A. *ChemBioChem*, **2011**, *12*, 2623-2629. (e) Weis, S.; Shafiq, Z.; Gropeanu, R. A.; del Campo, A. *J. Photoch. Photobio. A* **2012**, *241*, 52-57. (f) Sainlos, M.; Iskenderian-Epps, W. S.; Olivier, N. B.; Choquet, D.; Imperiali, B. *J. Am. Chem. Soc.* **2013**, *135*, 4580-4583. (g) Sainlos, M.; Iskenderian-Epps, W. S.; Olivier, N. B.; Choquet, D.; Imperiali, B. *J. Am. Chem. Soc.* **2013**, *135*, 4580-4583. (h) Nomura, A.; Uyeda, T. Q. P.; Yumoto, N.; Tatsu, Y. *Chem. Commun.* **2006**, 3588-3590. (i) Pan P.; Bayley, H. *FEBS Lett.* **1997**, *405*, 81-85. (j) Lawrence, D. S. *Curr. Opin. Chem. Biol.* **2005**, *9*, 570-575. (k) Karas, J. A.; Scanlon, D. B.; Forbes, B. E.; Vetter, I.; Lewis, R. J.; Gardiner, J.; Separovic, F.; Wade, J. D.; Hossain, M. A. *Chem. Eur. J.* **2014**, *20*, 9549-9552. (l) Kotzur, N.; Briand, B.; Beyermann, M.; Hagen, V. *Chem. Commun.* **2009**, 3255-3257.
- (8) (a) Ohmuro-Matsuyama, Y.; Tatsu, Y. *Angew. Chem. Int. Ed.* **2008**, *47*, 7527-7529. (b) Jiménez-Balsa, A.; Pazos, E.; Martínez-Albaronedo, B.; Mascareñas, J. L.; Vázquez, M. E. *Angew. Chem. Int. Ed.* **2012**, *51*, 8825-8829. (c) Grunwald, C.; Schulze, K.; Reichel, A.; Weiss, V. U.; Blaas, D.; Piehler, J.; Wiesmuller, K. H.; Tampe, R. *Proc. Nat. Acad. Sci. U. S. A.* **2010**, *107*, 6146-6151, (d) Nandy, S. K.; Agnes, R. S.; Lawrence, D. S. *Org. Lett.* **2007**, *9*, 2249-2252. (e) Johnson, E. C.; Kent, S. B. *Chem. Commun.* **2006**, 1557-1559.
- (9) Mosquera, J.; Sánchez, M. I.; Mascareñas, J. L.; Vázquez, M. E. *Chem. Commun.* **2015**, *51*, 5501-5504.
- (10) Kalka, K.; Merk, H.; Mukhtar, H. *J. Am. Acad. Dermatol.* **2000**, *42*, 389-413.

- (11) (a) Brash, D.; Rudolph, J.; Simon, J.; Lin, A.; Mckenna, G.; Baden, H.; Halperin, A.; Ponten, J. *Proc. Natl. Acad. Sci. U.S.A.* **1991**, *88*, 10124–10128. (b) Protic-Sabljić, M.; Tuteja, N.; Munson, P.; Hauser, J.; Kraemer, K.; Dixon, K. *Mol. Cell. Biol.* **1986**, *6*, 3349–3356. (c) Steven, L. J. *Phys. Med. Biol.* **2013**, *58*, R37-R61. (d) Hopkins, S. L.; Siewert, B.; Askes, S. H. C.; Veldhuizen, P.; Zwier, R.; Heger, M.; Bonnet, S. *Photochem. Photobiol. Sci.* **2016**, *15*, 644-653.
- (12) (a) Desgrosellier, J. S.; Cheresch, D. A. *Nat. Rev. Cancer* **2010**, *10*, 9-22. (b) Auzzas, L.; Zanardi, F.; Battistini, L.; Burreddu, P.; Carta, P.; Rassu, G.; Curti, C.; Casiraghi, G. *Curr. Med. Chem.* **2010**, *17*, 1255-1299. (c) Mas-Moruno, C.; Fraioli, R.; Rechenmacher, F.; Neubauer, S.; Kapp, T. G.; Kessler, H. *Angew. Chem. Int. Ed.* **2016**, *55*, 7048-7067.
- (13) Arosio, D.; Casagrande, C. *Adv. Drug Deliver. Rev.* **2016**, *97*, 111-143.
- (14) (a) Mukhopadhyay, S.; Barnés, C. M.; Haskel, A.; Short, S. M.; Barnes, K. R.; Lippard, S. J. *Bioconjugate Chem.* **2008**, *19*, 39-49. (b) Graf, N.; Bielenberg, D. R.; Kolishetti, N.; Muus, C.; Banyard, J.; Farokhzad, O. C.; Lippard, S. J. *ACS Nano*, **2012**, *6*, 4530-4539. (c) Yuan, Y.; Kwok, R. T. K.; Tang, B. Z.; Liu, B. *J. Am. Chem. Soc.* **2014**, *136*, 2546-2554. (d) Barragán, F.; López-Senín, P.; Salassa, L.; Betanzos-Lara, S.; Habtemariam, A.; Moreno, V.; Sadler, P. J.; Marchán, V. *J. Am. Chem. Soc.* **2011**, *133*, 14098-14108. (e) Massaguer, A.; González-Cantó, A.; Escribano, E.; Barrabés, S.; Artigas, G.; Moreno, V.; Marchán, V. *Dalton Trans.* **2015**, *44*, 202-212. (f) Gandioso, A.; Shaili, E.; Massaguer, A.; Artigas, G.; González-Cantó, A.; Woods, J. A.; Sadler, P. J.; Marchán, V. *Chem. Commun.* **2015**, *51*, 9169-9172. (g) Soler, M.; Feliu, L.; Planas, M.; Ribas, X.; Costas, M. *Dalton Trans.* **2016**, *45*, 12970-12982.
- (15) (a) Hagen, V.; Dekowski, B.; Kotzur, N.; Lechler, R.; Wiesner, B.; Briand, B.; Beyerman, M. *Chem. Eur. J.* **2008**, *14*, 1621-1627. (b) Fournier, L.; Aujard, I.; Le Saux, T.; Maurin, S.; Beaupierre, S.; Baudin, J.-B.; Jullien, L. *Chem. Eur. J.* **2013**, *19*, 17494-17507.
- (16) Schmidt, R.; Geissler, D.; Hagen, V.; Bendig, J. *J. Phys. Chem. A* **2007**, *111*, 5768-5774.
- (17) (a) Kirpichenok, M. A.; Gorozhankin, S. K.; Granberg, I. I. *Chem., Heterocycl. Compd.* **1988**, 611-616. (b) Fournier, L.; Gauron, C.; Xu, L.; Aujard, I.; Le Saux, T.; Gagey-Eilstein, N.; Maurin, S.; Dubruille, S.; Baudin, J.-B.; Bensimon, D.; Volovitch, M.; Vríz, S.; Jullien, L. *ACS*

- Chem. Biol.* **2013**, *8*, 1528-1536. (c) Fonseca, A. S. C.; Soares, A. M. S.; Gonçalves, M. S. T.; Costa, S. P. G. *Tetrahedron* **2012**, *68*, 7892-7900. (d) Yamazoe, S.; Liu, Q.; McQuade, L. E.; Deiters, A.; Chen, J. K. *Angew. Chem. Int. Ed.* **2014**, *53*, 10114-10118.
- (18) Jesberger, M.; Davis, T. P.; Barner, L. *Synthesis* **2003**, 1929–1958.
- (19) Subirós-Funosas, R.; El-Faham, A.; Albericio, F. *Tetrahedron*, **2011**, *67*, 8595-8606.
- (20) (a) Michels, T.; Dölling, R.; Haberkorn, U.; Mier, W. *Org. Lett.* **2012**, *14*, 5218-5221. (b) Subirós-Funosas, R.; El Faham, A.; Albericio, F. *Pept. Sci.* **2012**, *98*, 89-97.
- (21) Gross, A.; Habig, D.; Metzler-Nolte, N. *ChemBioChem* **2013**, *14*, 2472-2479.